

New simulation tools allow exact predictions of the microstructure after heat treatment of ADI (Photo: ACTech)

Authors: Dipl.-Phys. Ole Köser and Alain Jacot, Calcom ESI, Lausanne, Dr.-Ing. Uwe Getzlaff, ACTech GmbH, Freiberg

Modeling the heat treatment of ausferritic ductile iron

Ausferritic ductile iron (ADI) combines the freedom of the molding style of cast iron with the strengths of steel. ADI forms by heat treatment of nodular cast iron. To take full advantage of the technical potential of this material, extensive controls of the casting and the heat treatment processes are required. The authors describe an integrated approach of experimental studies and modelling for optimum process design. The simulation tools developed permit exact predictions of the microstructure due to the heat treatment. If certain suitable technical parameters are observed, an ausferritic microstructure without pearlite, martensite and bainite can be obtained. The parts produced had very good reproducible mechanical properties distinctly better than the applicable limits

Ausferritic ductile iron (ADI) forms when nodular cast iron is subjected to heat treatment. The material was standardized in 1990 with the following characteristics:

- » Tensile strength R_m : 850 MPa to 1600 MPa;
- » Tensile yield strength $R_{p0.2}$: 550 MPa to 1300 MPa;
- » Elongation at fracture A_5 : 10% to 1%.

In contrast with standards DIN EN 1564 (1997) and ISO 17804 (2005), standard SAE J2477 (2004) also contains requirements for the casting process, microstructure and heat treatment. Following the studies undertaken by ACTech GmbH, Freiberg/Germany, under the Precision Cast Project funded by the „Unternehmen Region“ BMBF innovation initiative of the German

Ministry of Education and Research in which six firms and two universities cooperated, the following requirements on the quality of the casting, i.e. the original microstructure, were defined:

- » Uniform composition of the liquid metal;
- » Suitable inoculant;
- » Uniform pearlite/ferrite ratio;
- » Maximum porosity of 0.5%;

- » Minimum of 100 spherulites per mm²;
- » Minimum nodularity of 90%;
- » Minimized segregation and carbides (max. 0.5% carbides).

A reproducible heat treatment produces an ausferrite with the following features:

- » No pearlite;
- » No martensite;
- » No bainite;
- » Max. 0.5% carbides;
- » Residual austenite content of 20 to 40% (depending on grade).

If these quality parameters are met, the strength of the ausferrite is distinctly higher than that specified by applicable standards (Figure 1).

Thus, ausferritic ductile iron (ADI) combines the freedom of molding of cast iron with the strength of steel. The range of applications which this entails is grossly underutilized because many developers are uncertain as far as the design of ADI components is concerned. The strength characteristics and the fracture behaviour of ADI were studied by several authors [1, 2]. The transformation processes have also been described as functions of the distribution of carbon and the alloying constituents [3, 4, 5]. The austenitizing time and the austenitizing temperature as well as the austempering time and the austempering temperature are under technological control. Likewise, the required equipment for the quick transfer from the austenitizing furnace

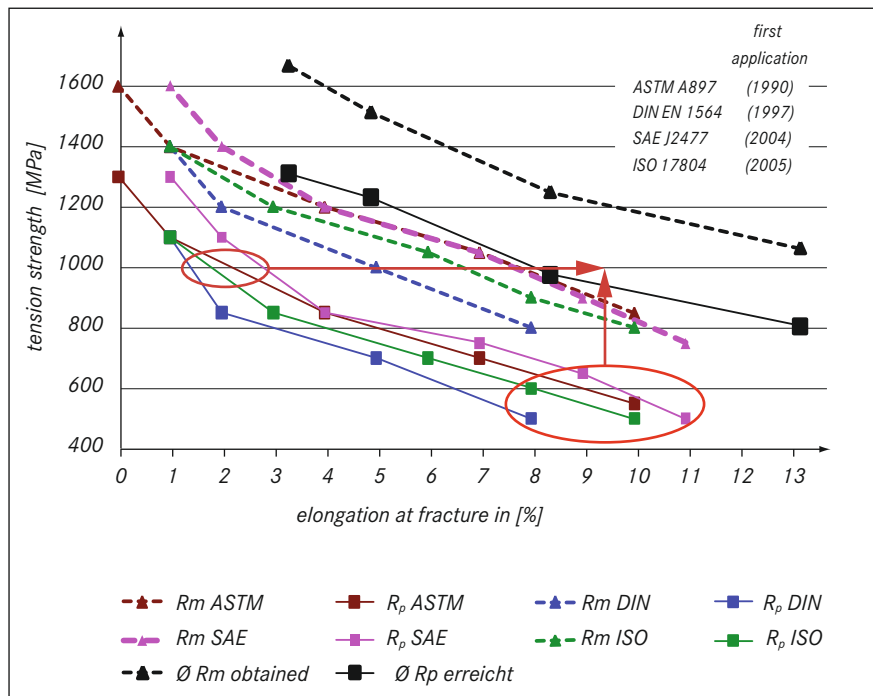


Figure 1: ADI grades – standards and values obtained. The obtainable ADI strengths are far higher than the standard levels

to the austempering bath is in place. From the practical angle, the cooling rate inside a massive part is the critical process that determines the specific quality of the material in an ADI part.

Figure 2 shows the principal steps of the heat treatment process and the different microstructures which can occur during heat treatment. At the beginning of treatment, the part is heated to austenitizing temperature (distinctly above the PSK line in the iron carbon diagram, e.g. 900 °C) for complete austenitization of the micro-

structure. Then the part is quenched to a bainite temperature. This process must proceed at high speed to avoid formation of pearlite. However, the part should not be quenched too much as this would promote the formation of martensite. The transformation kinetics can be controlled systematically by the alloying elements nickel, molybdenum and/or copper. The transformation of the microstructure to ausferrite occurs at a holding temperature around 300 °C. Long holding times should be avoid-

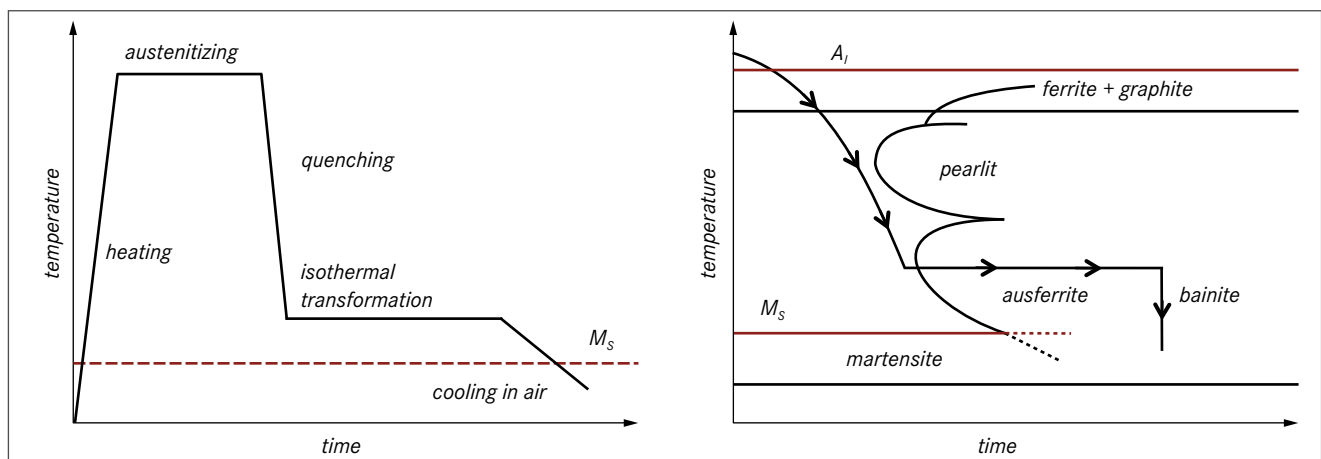


Figure 2: Principal phases of the heat treatment of ADI and microstructure components

ed as this would cause the formation of bainite with unfavourable mechanical properties.

The transformation of the microstructure can be defined and controlled by simulation for every part right from the development phase. Simulation enables the designer to predict the temperature-time behaviour at different locations in a part. By coupling heat simulation with models for alloy-dependent transformation kinetics, the local microstructure distribution can be predicted with high accuracy. This article looks at the experimental and theoretical aspects of such an approach and explains how

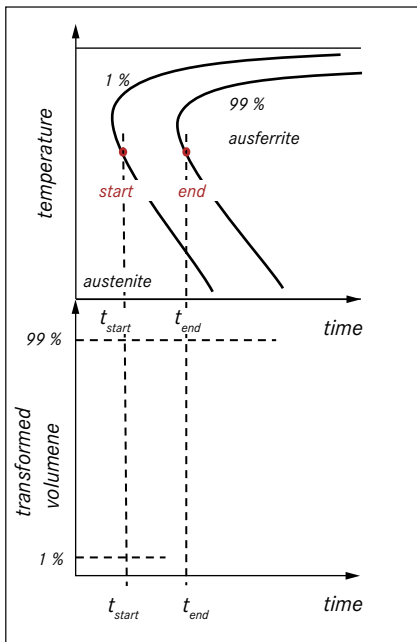


Figure 3: Structure transformation at constant temperature

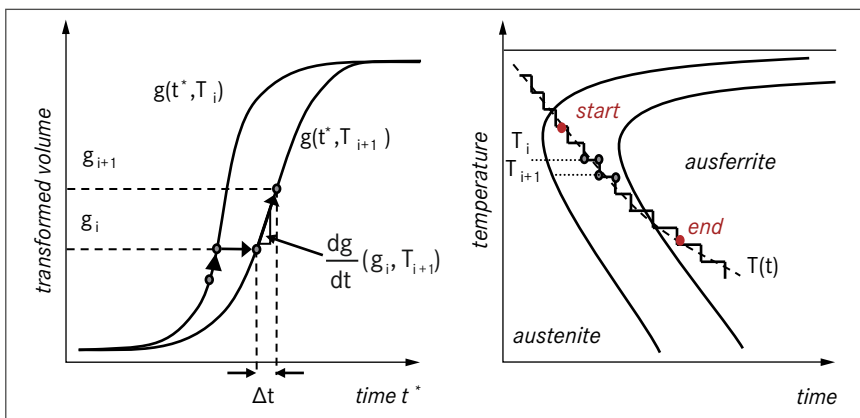


Figure 4: Structure transformation with any cooling curves based on time-related discretization

the process simulation can be applied successfully to part development and production planning.

Theoretical background for the representation of structural transformation

Microstructure transformation of the type known from the heat treatment of ADI can be plotted in T-T-T (time-temperature transformation) diagrams. A difference is made between isothermal and continuous T-T-T diagrams. A series of T-T-T diagrams for cast nodular cast iron was published in [6]. Isothermal diagrams describe the transformation of one microstructural state to another at a constant temperature. The kinetics of the transformation can be described by the KJMA (Kolmogorov-Johnsen-Mehl-Avrami-) theory as follows:

$$g(t, T) = \exp \left[- \left(\frac{t}{\tau(T)} \right)^{n(T)} \right] \quad (1)$$

In the above equation, t is the time, T the temperature, g the transformed volume portion, τ the characteristic transformation time, and $n(T)$ an exponent characterizing nucleation and the growth mechanism. Typically, the parameters of equation (1) $t(T)$ and $n(T)$ are determined by t_{start} corresponding to 1% and t_{end} corresponding to 99% structure transformation as follows:

$$0,01 = 1 - \exp \left[- \left(\frac{t_{start}}{\tau(T)} \right)^{n(T)} \right] \quad (2a)$$

$$0,99 = 1 - \exp \left[- \left(\frac{t_{end}}{\tau(T)} \right)^{n(T)} \right] \quad (2b)$$

Figure 3 is a schematic representation of corresponding isothermal transformation behaviour of austenite to ausferrite at different temperatures.

Real heat treatment processes do not proceed at constant temperature. For this reason, it is important to extend the theoretical description to all cooling curves. **Figure 4** illustrates the principle by which cooling processes of this type can be simulated. The cooling curve is divided into finite time increments. The volume portion increases at each horizontal portion of the curve as a function of the isothermal connection at that moment, the temperature and the time increment. The vertical portion of the increment represents the acceptance of the calculated new volume portion as starting value for the next time increment. The increment in each case can be described by the derivation of the transformation kinetics by the following equation (cf. Figure 4):

$$g_{i+1} = g_i + \frac{dg}{dt} (g_i, T_{i+1}) (t_{i+1} - t_i) \quad (3)$$

and, respectively

$$g_{i+1} = g_i + \frac{\frac{dg}{dt} (g_i, T_{i+1}) + \frac{dg}{dt} (g_i, T_i)}{2} \cdot (t_{i+1} - t_i) \quad (4)$$

The derivation of the transformation kinetics is obtained from (1) as follows:

$$\frac{dg}{dt} (g_i, T_{i+1}) = (1 - g_i) = \frac{n(T_{i+1})}{\tau(T_{i+1})} \left(\text{Ln} \frac{1}{1 - g_i} \right) \quad (5)$$

The connections shown above were integrated in the microstructure model of ProCAST for the different phase transformations.

Experimental studies

Experimental studies were made in three categories:

- » Examination of the transformation kinetics by dilatometer measurements;

- » Determination of the process parameters during the heat treatment; and
- » Evaluation of the microstructure formed (depending on geometry, alloy and process parameters).

The dilatometer measurements by which the transformation kinetics was determined were made at the Institute for Iron and Steel Technology at the Technical University Bergakademie Freiberg in Germany. Several technically interesting alloys of which parts of different massiveness can be produced were examined. The samples were austenitized for a sufficient length of time. To determine the map for the continuous T-T-T diagram, the specimens were cooled at defined rates from 50 K/s to 0.2 K/s after austenitizing. To determine the map for the isothermal T-T-T diagrams, the samples were quenched at defined temperatures from 240 °C to 520 °C after austenitizing and then held for up to 100 h. The beginning and end of the transformation processes are revealed by the change of length. At the end, the structure of each specimen was examined. The continuous tests were repeated for points of interest, and stopped by quenching at the end of the interesting time and the microstructure examined again. The dilatometer tests provide the basis of the curves shown in Figure 3 for the determination of parameters required for simulation.

Heat treatment comprises the process steps of heating, austenitizing, quenching, isothermal transformation and cooling (cf. Figure 2). The steps of heating, austenitizing, isothermal transformation and cooling take from half an hour to several hours. Quenching, on the other hand, is a process of only a few seconds' duration. The geometry of a part is very important for the quenching process whereas it has virtually no effect on the other steps.

For a simulation of the heat treatment, it is sufficient to assume complete austenitization of the microstructure at the end of the austenitizing time if a sufficiently long austenitizing time is observed in practice. The austenitizing temperature is the only remaining process parameter. This temperature is maintained exactly by all

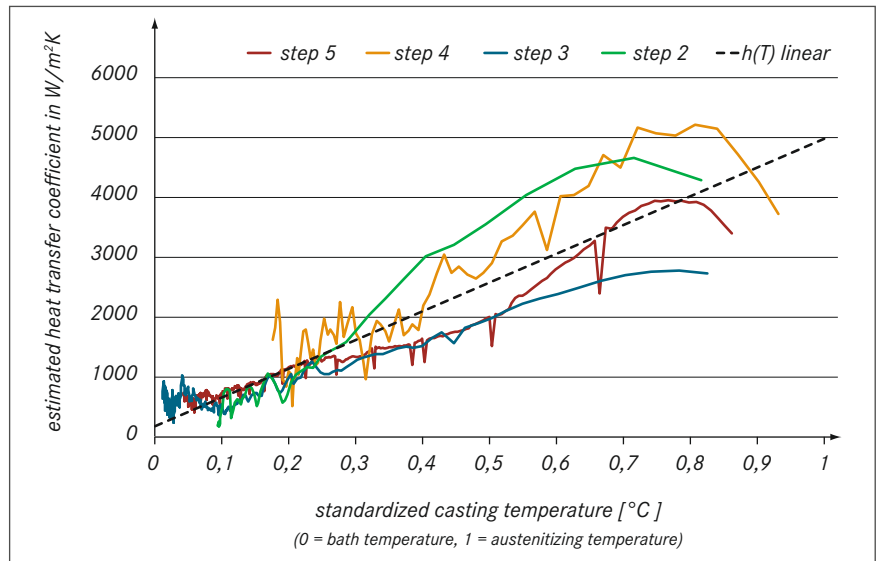


Figure 5: Heat transition coefficient as function of the casting temperature

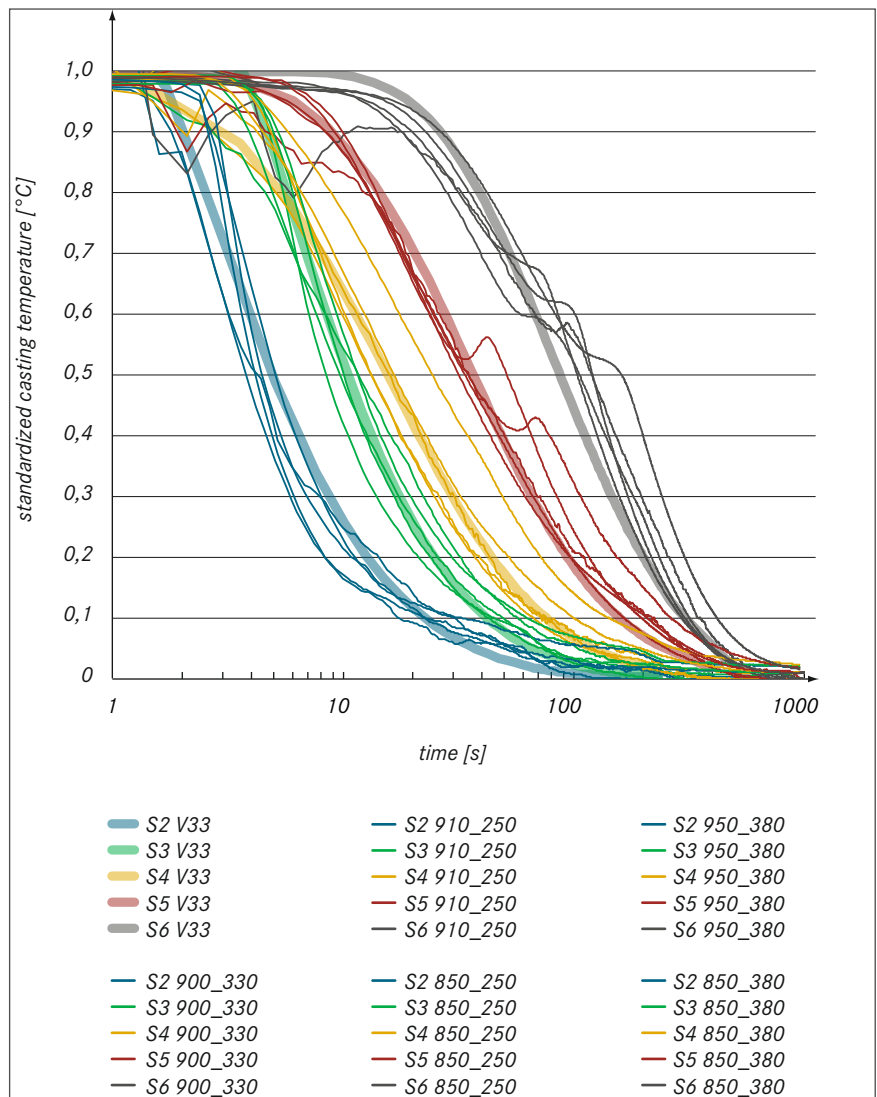


Figure 6: Cooling in the bath – a comparison between measurement and simulation

■ SIMULATION

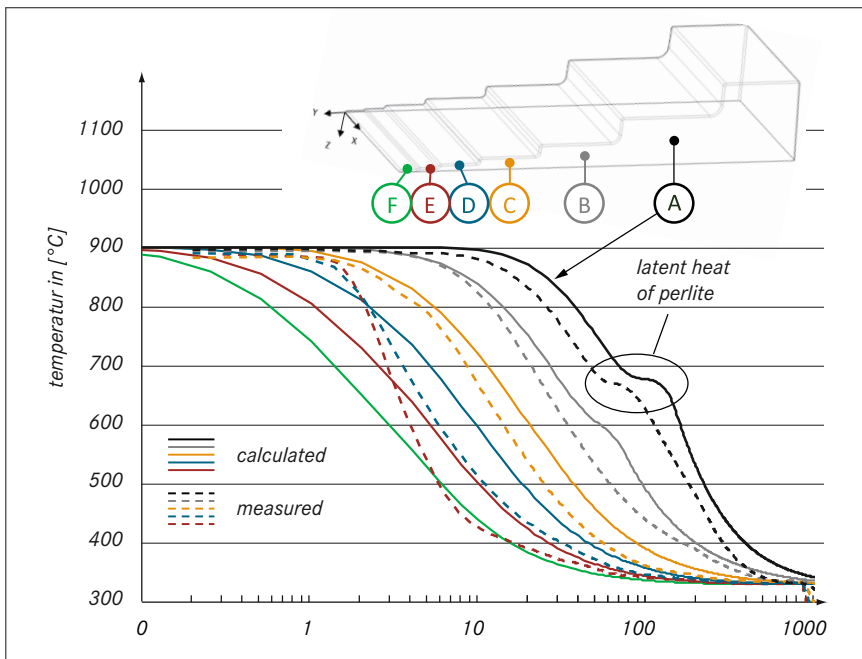


Figure 7: Comparison of measured and modelled cooling curves in the salt bath at 330 °C

common heat treatment systems and is therefore known for the simulation.

For quenching, the part is lowered into the transformation bath directly from the furnace above the bath. If this

happens quickly enough, it can be assumed for the simulation that the component is at austenitizing temperature at time zero and the boundary condition corresponds to the heat trans-

fer between the part and the transformation bath. The bath temperature is known and can be controlled reliably by the technical equipment. The heat transfer coefficient h depends on the composition and the chemistry of the bath, the recirculation flow in the bath as well as on the bath temperature T_B and the part temperature T_P . This heat transfer coefficient must be determined for concrete technical conditions.

To determine the heat transfer coefficient during quenching, temperature measurements were performed during the heat treatment at bath temperatures between 250°C and 380°C and austenitizing temperatures between 850 °C and 950 °C. For this, step bar test castings and balls of different size were quenched. The temperature profile in a ball can be characterized analytically both in terms of time and site [7]. As the heat transfer coefficient is a function of the bath temperature and the part temperature, and because of the release of latent heat during pearlite formation, no direct calculation of the heat transfer coefficient $h(T_P, T_B)$

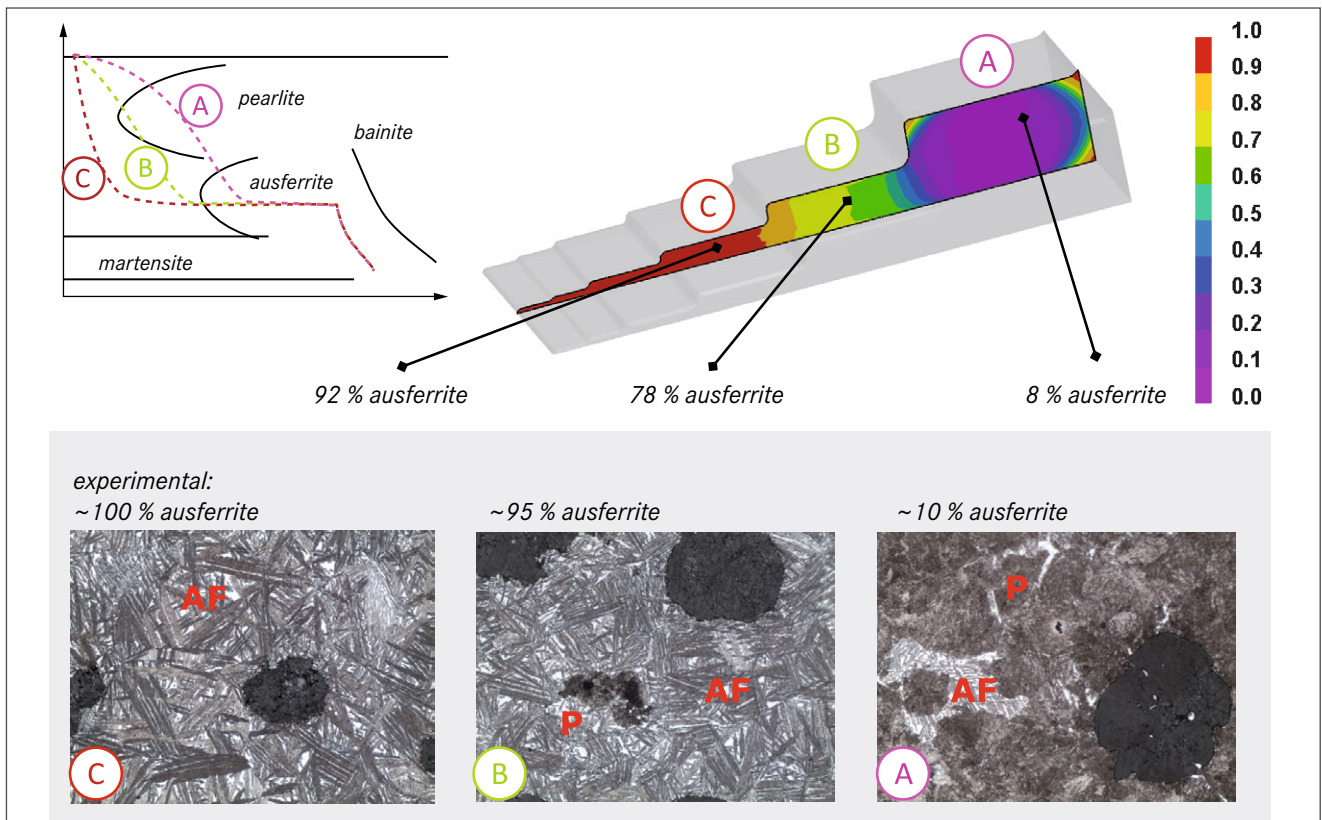


Figure 8: Comparison of experimental microstructure distribution and that determined by simulation

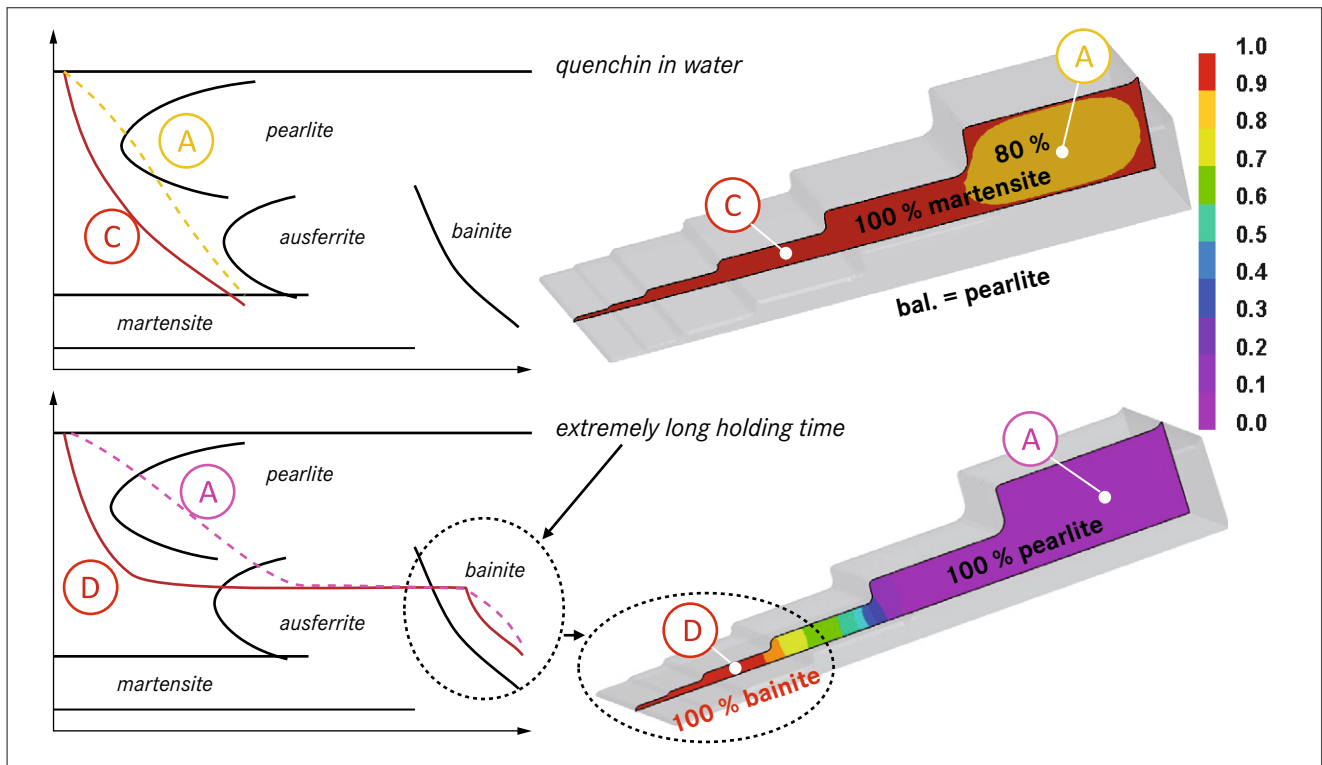


Figure 9: Formation of martensite and bainite under unfavourable process parameters

from the temperature values is possible. Also, the effect of the finite heat conduction of the casting and the local temperature gradient caused by it cannot be neglected. Empirically, the heat transfer coefficient is of the order of $h \approx 1000 \text{ W}/(\text{m}^2 \cdot \text{K})$. For a heat conductivity of nodular cast iron of approx. $\lambda \approx 32 \text{ W}/(\text{m} \cdot \text{K})$ and a material thickness of 32 mm between the surface and the thermocouple, a heat transmission coefficient of $U_p \approx 1000 \text{ W}/(\text{m}^2 \cdot \text{K})$ is also obtained. The effect of the heat transfer coefficient right into the thermocouple must be considered by all means.

Experimental tests with step bar test castings were carried out for calibrating the simulation. A step bar test casting is particularly suitable for such examinations because the cooling curves vary according to the different thicknesses. Applying a simplified estimation of the heat transfer coefficient h in the first step, the variables on which that coefficient depended and how these variables can be characterized qualitatively was studied. The total heat transmission coefficient U_{ges} is obtained from the heat flow

$$Q = V \cdot \rho \cdot c_p \cdot \frac{dT_p}{dt} \quad (6a)$$

$$Q = A \cdot U(t)_{ges} \cdot (T_p(t) - T_B) \quad (6b)$$

with

$$U(t)_{ges} \cong \frac{V \cdot \rho \cdot c_p}{A} \cdot \frac{dT_p}{T_p(t) - T_B} \cdot \frac{dT_p}{dt} \quad (7).$$

The heat transfer coefficient h can be estimated from the measurement of the total heat transfer coefficient U_{ges} with consideration of the heat transfer coefficient U_p between surface and thermocouple from

$$h(t) \cong \frac{1}{\frac{1}{U(t)_{ges}} - \frac{1}{U(t)_p}} \quad (8).$$

The heat transfer coefficient $h(t)$ can be presented as $h(T_p)$ for different bath temperatures T_B as a function of the casting temperature $T_p(t)$. This was done in **Figure 5** in standardized representation for a test with a bath temperature.

The estimated heat transfer coefficients show that the choice of a linear parameter function $f(T_p, T_B)$ for $h(T_p,$

$T_B)$ is sufficient, and served as starting point for the determination of $h(T_p, T_B)$ by simulation and parameter optimization in which the deviation between the simulated temperatures $T_{Sim\ i,j}$ and the measured temperatures $T_{Mess\ i,j}$ becomes minimum for all tests k , all measuring points j and all time increments i .

$$\sum_{i,j,k} (T_{Sim\ i,j,k}(h(f(T_p, T_B))) - T_{Mess\ i,j,k})^2 \rightarrow \min \quad (9)$$

The standardized presentation of the result for all tests is given in **Figure 6**. The thick lines are the simulated events; the thin lines were measured; however, at this point, the simulation was still performed without structural transformation.

Validation of the simulated microstructure distributions by the example of a step bar test casting

The calibration and validation of the coupled thermal and microstructure simulation were performed in two steps. At first, the temporal temperature

SIMULATION

curves were plotted and checked against simulated data. In the second step, the local microstructure was examined and considered for the simulation.

Figure 7 shows the measured temperature plot (dashed lines) in comparison with the simulated temperatures (solid line). Pearlite forms in the massive region of the specimen due to slow cooling. The associated release of latent heat is expressed by a plateau in

unstructured area is typical of pearlite (marked P in Figure 8). The light grey, needle-shaped area represents ausferrite (marked AF in Figure 8). Shown above the metallographic specimens in Figure 8 is the ausferrite portion at different positions in the step bar test casting predicted by the simulation; seen on the top left is the schematic procedure of the heat treatment for an explanation of the results.

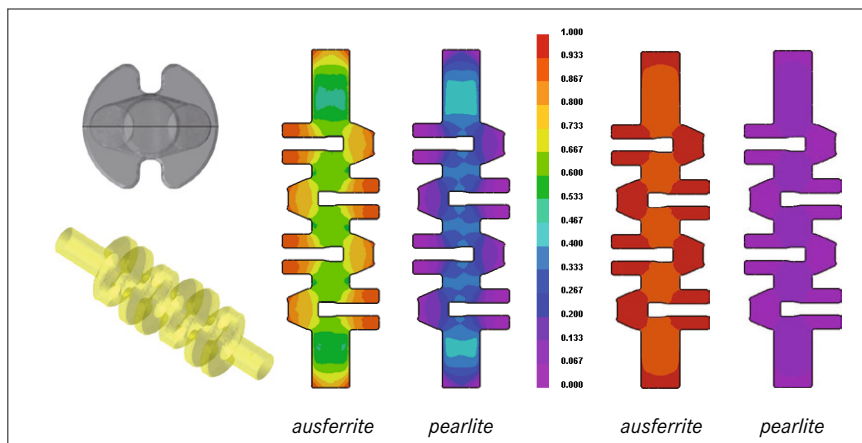


Figure 10: Result of modelling with the example of a crankshaft – proportion of the microstructure components

the cooling measurement curve (black curve see section A in Figure 7) in the region between 600 and 700 °C. To be able to translate this behaviour in the simulation, the energy generated by the formation of pearlite is transferred from the microstructure module to the thermal solver. The behaviour observed during the measurement is reflected very well in the modelled data. Next, a comparison between modelled structure distributions and distributions obtained by metallographic examinations was made on the basis of the calibrated temperature distributions. The results of this comparison are presented for a step bar test casting with 0.8% nickel in **Figure 8**.

Three different regions were selected for the metallographic examinations: Region A as the region of slowest cooling, region B with a medium cooling rate, and a thin-wall region C with very fast cooling. Three different phases can be observed in the metallographic specimens: The round, dark grey areas represent the graphite nodules. The grey

The step bar test casting is very thick in region A so that cooling takes place very slowly there. The cooling curve clearly passes through the pearlite area, i.e., much of the austenite converts to pearlite. Consequently, little material remains for conversion from austenite into ausferrite. This explains the smaller share of ausferrite (of the order of 10 %) observed in the experimental and the simulated results. Looking at the cooling curve marked B, it will be seen that the pearlite area is only traversed marginally. Consequently, little pearlite forms and most of the austenite is converted to ausferrite. C is located in the thin-wall region where cooling is fast. So no pearlite forms and complete conversion to the required ausferrite phase can be obtained. In summary, it can be stated that the quality of the ausferrite share predicted by simulation agrees well with the experimental results. It goes without saying that a part with such a high ratio of volume/surface area would be cast with a higher alloy than 0.8% nickel to obtain complete ausferritization.

Effects of unfavourable process parameters

The simulation results presented above focused on the prediction of pearlite and ausferrite. In addition, the martensite and bainite phases can occur during the heat treatment process. Because both phases have adverse mechanical properties and can be the result of the poor design of the heat treatment process, the microstructure module of the simulation software was extended to be able to consider the formation and kinetics of these phases.

Figure 9 illustrates the effects of two wrong heat treatment programs selected with intention. In the top part, the step bar test casting is not quenched in the oil or salt bath but cooled to room temperature by immersion in water. As a consequence of this, martensite forms in region C. The martensite formation is incomplete in region A because pearlite also forms during the slow cooling rate and converts to martensite. In the second case (bottom in Figure 9) the test casting is quenched in the oil or salt bath, but the holding time is too long. As a result of this the ausferrite in region D turns into bainite. No bainite formation is observed in region A because the slow cooling here causes pearlite to form, which does not convert into bainite.

Practical application

Crankshafts are exposed to high dynamic stress at operating temperatures constantly below 200 °C. Occasionally, expensive forged steel shafts are installed in high-output engines and lower priced crankshafts of nodular cast iron in engines with lower output. ADI crankshafts are nearly perfect for the medium output range. **Figure 10** shows the model of the structure distribution by the example of a crankshaft, an alloy with 1.1 % nickel on the left and an alloy with 2 % nickel on the right. Pearlite would have been tolerable in the core area of the part. However, the simulation shows that in the 1.1% nickel crankshaft pearlite forms as far as into the notches between the main bearings and the crank webs, which are subject to high mechanical stress, and therefore the higher nickel alloy should be chosen.

Summary

ADI castings permit a high degree of design freedom and are of high strength. The alloy and the geometry of the ADI parts must be matched accurately to ensure full hardening during heat treatment. The transformation kinetics and dilatometer measurements were deter-

mined for relevant alloys and the casting simulation system ProCast implemented. The simulation results were validated by technological samples. With this tool the microstructure after the heat treatment can be predicted and the correct alloy chosen already at the part development stage.

www.esi-group.com
www.actech.de

References

www.giesserei-verlag.de/cpt/references